Lawrence Berkeley National Laboratory

Title
VIBRATIONAL SPECTRA AND NORMAL COORDINATE ANALYSIS OF NEPTUNIUM (IV) BOROHYDRIDE AND NEPTUNIUM (IV) BORODEUTERIDE

Permalink

Author
Banks, Rodney H.

Publication Date
2013-06-27

Lawrence Berkeley Laboratory
UNIVERSITY OF CALIFORNIA

Materials & Molecular Research Division

VIBRATIONAL SPECTRA AND NORMAL COORDINATE ANALYSIS OF
NEPTUNIUM (IV) BOROHYDRIDE AND NEPTUNIUM (IV) BORODEUTERIDE

Rodney H. Banks and Norman Edelstein
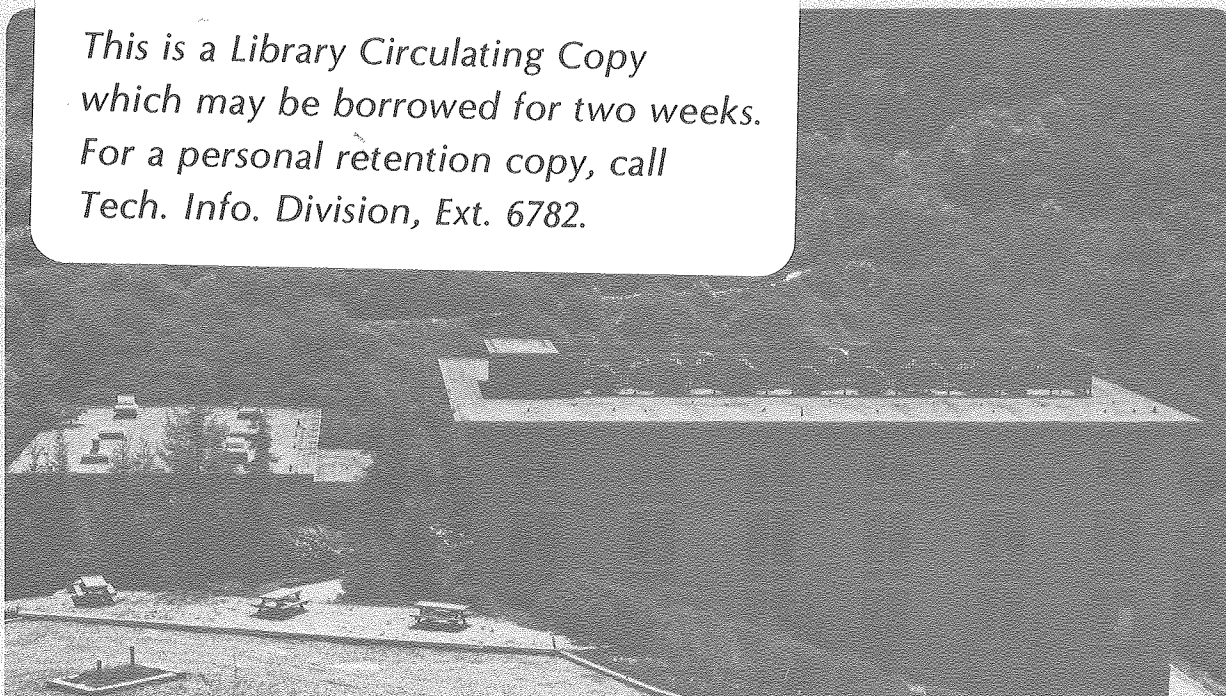
June 1980

DISCLAIMER

LBL 10901

Vibrational Spectra and Normal Coordinate Analysis of Neptunium (IV) Borohydride and Neptunium (IV) Borodeuteride

Rodney H. Banks* and Norman Edelstein

Materials and Molecular Research Division
Lawrence Berkeley Laboratory
and
Department of Chemistry
University of California
Berkeley, California 94720

June 1980

Abstract

Solid state, low temperature IR (25-7400 cm^{-1}) and Raman (100-2600 cm^{-1}) spectra were obtained for $Np(BH_4)_4$ and $Np(BD_4)_4$ from which most of the allowed fundamentals were assigned based on the T_d molecular structure. Those assignments were used in a normal coordinate analysis to derive a simple force field using 8 primary and 5 interaction constants. This field is very similar to those found for $Zr(BH_4)_4$ and $Hf(BH_4)_4$. Isotopic impurity, overtone, and combination bands were identified in the IR spectra with the help of the normal coordinate calculations. Near IR spectra of $Zr(BH_4)_4$ and $Zr(BD_4)_4$ were taken in the range 7400-4000 cm^{-1} and the observed absorption bands were assigned as either overtone or combination levels.

*Present address: Department of Chemistry, Argonne National Laboratory, Argonne, IL. 60439

Vibrational Spectra and Normal Coordinate Analysis of

Neptunium (IV) Borohydride and Neptunium (IV) Borodeuteride

Rodney H. Banks and Norman Edelstein

I. Introduction

Uranium borohydride, $U(BH_4)_4$, was the first tetrakis-borohydride known and was synthesized during the Manhattan project.[1] Subsequently $Hf(BH_4)_4$, $Zr(BH_4)_4$, and $Th(BH_4)_4$ were synthesized and their physical properties determined.[2] All four compounds are solids at room temperature, but $Hf(BH_4)_4$ and $Zr(BH_4)_4$ are appreciably more volatile than their actinide analogs. We have recently reported the syntheses of $Pa(BH_4)_4$, $Np(BH_4)_4$ and $Pu(BH_4)_4$.[3] As expected, $Pa(BH_4)_4$ has physical properties (melting point, sublimation temperature) intermediate to those of Th and U borohydrides. However $Np(BH_4)_4$ and $Pu(BH_4)_4$ are liquids at room temperature with vapor pressures very similar to those of $Hf(BH_4)_4$ and $Zr(BH_4)_4$ rather than the earlier actinide borohydrides.

The seven known metal tetrakis-borohydrides are all of the same symmetry in the gas phase[3-5] but in the solid state, exhibit three types of crystal structures.[6-9] Analyses of the vibrational spectra have been reported for the tetragonal, polymeric structure displayed by Th,[10] Pa,[11] and U[4,10,12] borohydrides and for the cubic monomeric structure shown by $Zr(BH_4)_4$[4,13] and $Hf(BH_4)_4$.[9,14] Those studies revealed that the vibrational spectra are highly dependent on solid state structure, and very noticeable spectral differences were observed for the two structure types. However in certain regions of the spectra it was not clear whether the effects of molecular geometry were primarily responsible for the noted dissimilarities or if other factors were also important. In

addition, the assignments of some spectral features remained doubtful and need further examination. Non-fundamental bands arising from combination and overtone transitions and normal modes involving isotopic impurity atoms were given little attention and IR spectra above 4000 cm^{-1} were not examined at all.

We report in this paper an analysis of the IR and Raman spectra of $Np(BH_4)_4$ and $Np(BD_4)_4$ which, like the analogous Pu compounds, display the third structure type, the tetragonal, monomeric structure.[6] An attempt was made to elucidate some of the uncertainties in the earlier analyses mentioned above and also to explain the origin of the non-fundamental bands seen in the IR spectra from 25-7400 cm^{-1} for $Np(BH_4)_4$ and in the near IR region for $Zr(BH_4)_4$. In doing so, it was found that the unobserved T_1 fundamentals and modes involving the less abundant ^{10}B atoms were very important, and required a heavy reliance on the normal coordinate calculations using the derived force field.

II. Experimental

Neptunium (IV) borohydride was prepared and purified as described previously.[3] Zirconium borohydride was synthesized by the reaction of Na_2ZrF_6 with liquid $Al(BH_4)_3$ at room temperature.[2] The borodeuterides were conveniently made by allowing a mixture of the metal borohydride vapor and dry, O_2-free D_2 gas to stand in a sealed glass reaction bulb at $25^{o}C$.[11] At 2-day intervals the bulb was cooled to -78°, evacuated, and refilled with another volume of D_2. After several such cycles the metal borodeuteride (> 99%D) was obtained in high yield.

Low temperature near IR spectra of $Np(BH_4)_4$, $Zr(BH_4)_4$, and $Zr(BD_4)_4$ were taken on a nitrogen-purged Cary 17 spectrophotometer in the

region 7400-4000 cm^{-1} (1.35-2.5μ). The borohydride compound was freshly sublimed from its storage tube held at -10°C into a degassed quartz optical cell. The cell was then sealed off and the solid borohydride was melted and collected into the lower optical section. Thin single crystals of $Zr(BH_4)_4$ (25 and 1000μ thick) and $Zr(BD_4)_4$ (1000μ thick) were vapor grown using the cold wire technique.[15] A $Np(BH_4)_4$ single crystal of 25μ path length was obtained by cooling the liquid very slowly to ∿ 150K in the optical dewar. All near IR spectra were taken at 2K.

For the region 4000-200 cm^{-1}, a N_2-flushed Perkin-Elmer 283 spectrophotometer was used. Room temperature gas phase spectra of $Np(BH_4)_4$ and $Np(BD_4)_4$ were taken of the sample vapor (∿ 6 Torr) contained in a 10 cm cell fitted with CsI windows. To obtain low temperature, solid state IR spectra in this region, the sample vapor was condensed as a thin film onto an inner CsI window cooled to 77K in a liquid nitrogen cryostat.

Far infrared spectra were obtained for $Np(BH_4)_4$ and $Np(BD_4)_4$ in the range 200-25 cm^{-1}. The cryostat employed was equipped with outer windows made of 2 mil-thick mica. The inner sample window was a thin, wedged sapphire disk cooled to 77K by a copper cold finger in contact with liquid nitrogen. The IR radiation was guided through the cryostat and into the detector via 1/2"O.D. brass light pipes which were kept evacuated during the runs. Absorptions due to window materials were subtracted out during data processing. A far infrared, 2-beam Michelson interferometer[16] was used to collect the data from which the spectra were obtained by computing the Fourier transforms of the truncated interferograms sampled at every 1/4 cm^{-1}.

Raman spectra were taken of $Np(BH_4)_4$ (2600-100 cm^{-1}) and $Np(BD_4)_4$ (2300-100 cm^{-1}) using a Ramanor HG, 2S spectrometer and the exciting

514.5 nm line of a Coherent Radiation Model CR-2 argon ion laser. The scattered light was analyzed at 90° to the incident beam with a J-Y double monochromator and detected by a photon counting system. The borohydride sample vapor was condensed as a thick polycrystalline layer onto a 77K cold finger housed in a 30 mm O.D. quartz tube. This spraying technique gave poor polarization results but was the only method tried which yielded acceptable peak intensities. The Raman polarized A_1 bands were easily identified by comparing the frequencies and intensities of our spectral lines to those in the Raman spectra of the Zr and Hf analogs.

III. Symmetry Classification of $M(BH_4)_4$ Normal Modes

A low temperature, single crystal x-ray diffraction study of $Np(BH_4)_4$[6] showed that the molecule is monomeric and the four borohydride ions are disposed tetrahedrally about the Np atom. The boron atoms are connected to the Np atom by triple hydrogen bridge bonds. There was no evidence that the symmetry of the molecule was lower than T_d. The molecular structure of $Np(BH_4)_4$ has the same basic geometry as that of $Zr(BH_4)_4$ and $Hf(BH_4)_4$[9,17] which were also found to be of T_d symmetry in the solid state by x-ray and neutron diffraction methods, respectively.

The 57 normal vibrational modes of a tetrahedral $M(BH_4)_4$ molecule can be classified according to their symmetry properties with $\Gamma_v = 4A_1 + A_2 + 5E + 5T_1 + 9T_2$. Only the T_2 modes are IR active and the A_1 (polarized), E, and T_2 modes are Raman active. Those vibrations which are of A_2 or T_1 symmetry are both IR and Raman inactive.

Some fundamentals give rise to overtone and combination bands which were seen in the vibrational spectra. Since combination bands are seldom observed in the ordinary Raman effect, only those which are symmetry allowed in the IR were considered here. Based on intensity arguments,[18]

difference bands were assumed to be unobservable. Only overtones of the T_1 and T_2 modes are IR active and those binary IR active combinations comprised of allowed parent fundamentals are $A_1 + T_2$, $E + T_2$, and $T_2 + T_2$. The active combination bands which involve the inactive A_2 or T_1 modes are $A_2 + T_1$, $E + T_1$, $T_1 + T_1$, and $T_1 + T_2$.

IV. <u>Infrared and Raman Spectra. 4000-25 cm^{-1} Region.</u>

The gas phase IR spectra of $Np(BH_4)_4$ and $Np(BD_4)_4$ are shown in Fig. 1. The low temperature, solid state IR spectra are given in Figs. 2 and 3 and the Raman spectra in Figs. 4 and 5. Complete listings of the absorption band frequencies, assignments, internal coordinate compositions, and qualitative descriptions of the spectral features for all spectra below 4000 cm^{-1} are given in Tables 1-3.

A. Assignment of Fundamental Vibrations.*

1. 2600-2500 cm^{-1} (2000-1900 cm^{-1}) Region

The highest energy fundamental vibrations are stretches of the boron and terminal hydrogen atoms. The four $B-H_t$ bonds transform as $A_1 + T_2$ where the A_1 mode is the in-phase vibration and the T_2 modes are the degenerate set of out-of-phase stretches.

Apart from coupling to other motions occurring in the molecule, these A_1 and T_2 modes should be similar in energy. A slightly broad band is seen in the Raman spectrum at 2557 cm^{-1} (H) and is assigned as $\nu_1^{A_1}$. The corresponding borodeuteride peak occurs at 1913 cm^{-1} ($\nu_1^{A_1}$) and is accompanied by a shoulder at 1925 ± 5 cm^{-1}. The gas phase IR spectra show strong bands at 2568 cm^{-1} (H) and 1922 cm^{-1} (D) with the latter having a shoulder at 1930 cm^{-1}. In the solid state, a strong, sharp singlet at 2551 cm^{-1} (H)

---

*See the Appendix to relate our numbering with earlier work.

and a sharp, intense absorption at 1912 cm^{-1}(D) adjacent to a weaker, well-resolved band at 1931 cm^{-1} are observed. The strong IR bands at 2551 cm^{-1} and 1912 cm^{-1} are assigned as $\nu_1{}^{T_2}$.

In terms of energy, these modes are far removed from all the others and are nearly pure $\nu BH_t(\nu BD_t)$ stretches with $\nu H/\nu D = 1.33$, indicating primarily hydrogen motion coupled to slight amounts of boron motion. As is observed in other metal borohydrides,[13,19] these vibrational states exhibit small matrix shifts to lower energies.

2. 2200-2000 cm^{-1} (1600-1500 cm^{-1}) Region

Normal modes giving absorption bands in this region are due to stretches of the boron and bridging hydrogen atoms. The set of twelve BH_b bonds transform as $A_1 + E + T_1 + 2T_2$ and four Raman and two IR bands are predicted to be observed in the spectra. In the gas phase, $Np(BH_4)_4$ shows two strong IR absorption bands at 2155 and 2084 cm^{-1} which experience matrix shifts to lower energies in the solid and appear at 2143 and 2069 cm^{-1}. These bands are assigned as $\nu_2{}^{T_2}$ and $\nu_3{}^{T_2}$, respectively. It is seen that $\nu_2{}^{T_2}$ is broader than $\nu_3{}^{T_2}$ due to the presence of a weak shoulder on $\nu_2{}^{T_2}$ at 2130 cm^{-1} which becomes well resolved in the solid state spectrum at 2110 cm^{-1}. The $\nu_3{}^{T_2}$ fundamental also splits in the solid with a separation of 10 cm^{-1}.

The Raman spectrum of $Np(BH_4)_4$ displays three bands instead of the predicted four at 2149, 2123, and 2070 cm^{-1} because $\nu_2{}^{A_1}$ at 2149 cm^{-1} overlaps with the $\nu_2{}^{T_2}$ peak seen in the solid state IR spectrum at 2143 cm^{-1}. The medium-intensity 2070 cm^{-1} Raman line, exhibiting a shoulder at 2060 cm^{-1}, corresponds to $\nu_3{}^{T_2}$ which was observed as a close doublet at 2069 and 2059 cm^{-1} in the IR spectrum. Since no IR coincidence is observed for the Raman

feature at $2123\,cm^{-1}$, its assignment as $\nu_1{}^E$ is straightforward.

The spectral pattern for $Np(BD_4)_4$ differs significantly from that just discussed for $Np(BH_4)_4$ in that three well separated IR bands and four Raman bands are observed. Similar behavior is also noted in the spectra of the analogous Zr,[13,20] Hf,[14,20] and U[12] compounds and a completely satisfactory explanation has yet to be found. Gas phase IR transitions occur at 1605, 1558, and 1526 cm^{-1} which sharpen and shift slightly to 1593, 1548, and 1516 cm^{-1} in the solid. Comparison of both energies and intensities of these bands with those of other metal tetrakis-borodeuterides[12,13] infers the assignment of 1516 cm^{-1} as $\nu_3{}^{T_2}$. The $\nu H/\nu D$ ratio for $\nu_3{}^{T_2}$ is 1.36 and is consistent with that expected for a νBH_b (νBD_b) stretching mode.

The four Raman bands are seen at 1619, 1592, 1549, and 1517 cm^{-1}. The strong, sharp peak at 1517 cm^{-1} is easily assigned as $\nu_2{}^{A_1}$[13,14] which is nearly coincident with its out-of-phase partner, $\nu_3{}^{T_2}(D)$, at 1516 cm^{-1}. Having a $\nu H/\nu D$ ratio of 1.31 and no strong IR incidence, the rather weak Raman line at 1619 cm^{-1} is tentatively assigned as $\nu_1{}^E$.

Since the remaining two Raman transitions at 1592 and 1549 cm^{-1} are practically at the same energies as the 1593 and 1548 cm^{-1} IR bands, they are identified as T_2 species, one of which is $\nu_2{}^{T_2}(D)$. Isotopic frequency ratios are not sufficiently sensitive here so both species are equally likely candidates. Intensity considerations, however, favor 1548 cm^{-1} (1549 cm^{-1}) as the fundamental vibration. The presence of the overtones of these νBD_b modes allows the identification of $\nu_2{}^{T_2}(D)$. In the solid state IR spectrum of $Np(BD_4)_4$ two weak but sharp peaks are observed at 3012 and 3074 cm^{-1}. As in the case of $Zr(BD_4)_4$, the $\nu_3{}^{T_2}$ fundamental produces an observable overtone, $2\nu_3{}^{T_2}$, seen at 3012 cm^{-1} in the spectrum of $Np(BD_4)_4$ ($2 \times \nu_3{}^{T_2} = 3032\ cm^{-1}$). The other νBD_b fundamental, $\nu_2{}^{T_2}$, being similar in internal coordinate composition to $\nu_3{}^{T_2}$, gives the overtone

at 3074 cm^{-1}. Assuming equal degrees of anharmonicity in $\nu_2^{T_2}$ and $\nu_3^{T_2}$, the frequency for $\nu_2^{T_2}$ can be calculated as

$$\nu_2^{T_2} = 1/2 \ (2\nu_2^{T_2} - 2\nu_3^{T_2}) + \nu_3^{T_2} = 1547 \ cm^{-1}.$$

This value is very close to those of the observed IR and Raman bands at 1548 and 1549 cm^{-1}, respectively, and these two bands are assigned as $\nu_2^{T_2}(D)$.

3. 1300-1050 cm^{-1} (950-800 cm^{-1}) Region

This spectral region is comprised of metal-hydrogen stretches and internal BH_4 bending motions. Each symmetrically equivalent set of internal coordinates, 12 MH_b, 12 H_bBH_b and 12 H_tBH_b transforms as $A_1 + E + T_1 + 2T_2$ and being similar in energy, combine to give complicated normal modes. Three IR and six Raman bands are expected to be observed.

The gas phase IR spectrum of $Np(BH_4)_4$ shows a strong broad band at 1240 cm^{-1}, a weaker one at 1122 cm^{-1}, and a number of shoulders visible on both. For the borodeuteride these modes are seen at 928 and 845 cm^{-1} where the latter is very weak. Infrared spectra for monomeric $U(BH_4)_4$[4,5,12] and $U(BD_4)_4$[12] show transitions at 1237 and 1121 cm^{-1} for the borohydride but only one band at 924 cm^{-1} for $U(BD_4)_4$. The three IR fundamentals are not distinguishable in the gas phase spectra where the broadness of the bands may cause the overlap of two modes which are close in energy. In contrast, $Zr(BH_4)_4$ and $Hf(BH_4)_4$ give different patterns and have bands which are well separated.

Differences in the solid state IR spectra between the Np and the Zr compounds are even more pronounced. The gas phase bands split into many sharper ones and the shoulders become clearly resolved. It is impossible with the

present data to correctly choose $\nu_4^{T_2}$, $\nu_5^{T_2}$, and $\nu_6^{T_2}$ but for the purpose of the normal coordinate calculation, any reasonable choice is satisfactory.

The broad 1240 cm^{-1}(H) gas phase absorption band experiences no observable matrix shift and in the solid divides into a strong, symmetrical doublet at 1247 and 1225 cm^{-1}. Although the weaker band at 1276 cm^{-1} corresponds well to $\nu_4^{T_2}$ at 1286 cm^{-1} in Zr(BH$_4$)$_4$, its low intensity does not favor this assignment and $\nu_4^{T_2}$ is assigned to the 1247 cm^{-1} peak. There is a Raman spectrum coincidence at 1230 cm^{-1}, so the 1225 cm^{-1} band is assigned as $\nu_5^{T_2}$. Matrix effects are most strongly observed for the 1122 cm^{-1}(H) gas phase band which is seen in the solid to be split into a doublet at 1159 and 1138 cm^{-1} where the most intense and least shifted peak (1138 cm^{-1}) is rather arbitrarily assigned as $\nu_6^{T_2}$. Overtone bands of these T$_2$ modes are observed in the solid state IR spectra but due to their broadness, they cannot help in locating the fundamental vibrations.

Similar behavior is noted in the Np(BD$_4$)$_4$ spectra. The strong gas phase absorption at 928 cm^{-1} becomes several equally intense bands at 941, 926, 917, and 910 cm^{-1} with the least shifted bands, 926 and 917 cm^{-1}, being assigned as $\nu_4^{T_2}$ and $\nu_5^{T_2}$. The very weak feature in the gas phase spectrum at 845 cm^{-1} sharpens in the solid state and moves to higher energy, 860 cm^{-1}, but unlike the borohydride case, does not split. It has a Raman spectrum correspondence at 863 cm^{-1} and is assigned as $\nu_6^{T_2}$.

In the Raman spectra, the $\nu_3^{A_1}$ modes occur at 1283 cm^{-1}(H) and 955 cm^{-1}(D) yielding νH/νD = 1.34. The E modes, ν_2^E and ν_3^E, are found at 1260 cm^{-1}(H), 905 cm^{-1}(D), and 1053 cm^{-1}(H), 795 cm^{-1}(D), respectively. These assignments

conform to those of the Zr and Hf compounds.

4. 600-450 cm^{-1} (450-400 cm^{-1}) Region.

At this point one A_1, two E, and three T_2 fundamentals need to be located and four Raman and two IR bands are expected in this spectral region. Metal-boron stretches transform as A_1 + T_2 and for these modes, $\nu H/\nu D$ ratios should be near unity. For the other E and T_2 modes, the most significant contributions are from δHBH and νMH_b coordinates and therefore should give larger $\nu H/\nu D$ ratios ≈ 1.3.

The νMB stretching vibrations are easily identified with the aid of their low $\nu H/\nu D$ ratios. Strong IR bands at 475 cm^{-1}(H) and 437 cm^{-1}(D) give $\nu H/\nu D$ = 1.087 and are assigned as $\nu_8^{T_2}$(H) and $\nu_7^{T_2}$(D). Their in-phase counterparts, $\nu_4^{A_1}$(H,D), are observed at 517 cm^{-1}(H) and 475 cm^{-1}(D) in the Raman spectra and give a similar $\nu H/\nu D$ ratio of 1.088. The νMB T_2 fundamentals are present only weakly as shoulders in the Raman spectra near the bases of the $\nu_4^{A_1}$ bands.

Spectral differences between the actinide and Zr, Hf compounds are also seen in this region but in the IR spectra only. A medium intensity band occurs at $\sim$400 cm^{-1} in each of the Zr, $Hf(BD_4)_4$ spectra but not in those of $U(BD_4)_4$ or $Np(BD_4)_4$. Previous assignments[13,14] for these extra bands near 400 cm^{-1} identified them as $\nu_8^{T_2}$(D) lying below the intense $\nu_7^{T_2}$(D) fundamental by about 80 cm^{-1}. The corresponding Zr, Hf borohydride modes, $\nu_7^{T_2}$(H), however were not assigned with certainty as they were observed to be extremely weak. It was pointed out[9,20] in earlier papers that the great intensity of the 400 cm^{-1} bands may be due to a Fermi resonance interaction of $\nu_8^{T_2}$(D) with another T_2 species such that resonance occurs only for the borodeuterides. Our examination of the $\nu H/\nu D$ ratios for the νMB modes of the actinide compounds, where this

phenomenon is absent, to those of Zr and Hf, suggests that the other interacting T_2 species is $\nu_7^{T_2}(D)$. The ratios for the νMB modes of Np are 1.087 (T_2) and 1.088 (A_1) are the same as those of U, 1.087 (T_2). The corresponding T_2 ratios for Zr and Hf relative to 1.087 reflect the degree of Fermi resonance for these vibrations since their A_1 ratios, 1.078 and 1.082, respectively, are nearly the same as those of U and Np. T_2 ratios close to 1.087 indicate little or no resonance and smaller values suggest that some resonance is occurring. The $\nu H/\nu D$ ratios for $\nu_8^{T_2}(H)$ and $\nu_7^{T_2}(D)$ are 1.043 for Zr and 1.026 for Hf. It is concluded that $\nu_7^{T_2}(H)$ and $\nu_8^{T_2}(D)$ for all compounds are inherently very weakly IR active and only the latter is observed for Zr, Hf$(BD_4)_4$ through the effects of Fermi resonance with $\nu_7^{T_2}(D)$. The lack of an observed state other than $\nu_7^{T_2}$ for Np$(BD_4)_4$ in the 450-350 cm^{-1} range precludes an assignment of $\nu_8^{T_2}(D)$.

The remaining fundamental in this region is ν_4^E. In the Raman spectra of the Zr and Hf compounds very weak lines were assigned as ν_4^E at 533 cm^{-1}(H) and 435 cm^{-1}(D) for Zr and tentative assignments were made for Hf at 570 cm^{-1}(H) and 430 cm^{-1}(D). No bands near those of Zr and Hf are noted in the Np Raman spectra. There is a very weak band at 639 cm^{-1}(H) but no firm assignments for ν_4^E can be made since the borodeuteride counterpart is missing.

5. 200-25 cm^{-1} Region

The last two fundamental vibrations found in this region are $\nu_9^{T_2}$ and ν_5^E which are comprised of δHMH and small amounts of δBMB bends. The Raman spectra show very strong bands at 168 cm^{-1}(H) and 154 cm^{-1}(D). Weaker peaks are observed at 141 cm^{-1}(H) and 121 cm^{-1}(D). A priori, either of a pair could be the E or T_2 fundamental since both species are symmetry allowed in the Raman spectrum. Both bands have approximately the same $\nu H/\nu D$ ratio

and the Teller-Redlich isotopic product rules are not very useful here as assignments are missing from each of the E and T_2 symmetry blocks.

Far infrared spectra of $Np(BH_4)_4$ and $Np(BD_4)_4$ (Fig. 3) show strong bands at 130 cm^{-1}(H) and 112 cm^{-1}(D). These bands correspond reasonably well to the Raman lines at 141 cm^{-1} and 121 cm^{-1} and can be assigned as $v_9^{T_2}$. The other, higher-energy Raman bands at 168 cm^{-1} and 154 cm^{-1} are identified as v_5^E. Our assignments agree with those made for the Zr and Hf compounds.

B. Teller-Redlich Isotopic Product Rules

The theoretical ratios[11,18] for the products of frequencies can be useful in checking a set of assignments. Usually observed frequencies give ratios slightly smaller than predicted theoretically due to effects of anharmonicity.[18]

The experimental Teller-Redlich ratio for the complete A_1 symmetry block is 2.77 and compares very favorably to the theoretical ratio of 2.82. Although the E and T_2 blocks are incomplete, assuming a reasonable ratio of 1.33 for the missing assignments gives ratios of 10.1 and 3.51 for the T_2 and E blocks respectively. Theoretical ratios are 11.58 and 3.99.

V. Normal Coordinate Analysis

The program NORCRD used to calculate frequencies and normal coordinates was devised by W. Gwinn[21] and later expanded to include least squares fitting, group theory, and other calculations by D. Reuter.[22] It sets up the normal coordinate problem in terms of mass-weighted Cartesian coordinates in which the kinetic energy matrix is a unit matrix and the potential energy matrix contains

the force constants in terms of bond distances and angles. In diagonalizing the $\underset{\sim}{V}$ matrix the frequencies and normal modes are obtained.

The molecular structure parameters used in the calculations were taken from the results of the low temperature x-ray structure study on $Np(BH_4)_4$.[6] Internal coordinate sets employed in this analysis were the $4BH_t$, $12BH_b$, $12MH_b$, and $4MB$ bonds; $12H_tBH_b$, $12H_bBH_b$, and $12H_bMH_b$ (triads of H_b's related by C_3) angles; and $36H_bBMB$ torsions. Variations in these sets were considered during the fitting process. The fundamental frequencies which were used as input to the program were given unit weight and are listed in Tables 2 and 3.

Since there are not as many observed spectral data as there are independent force constants, an approximate general valence force field was derived using a limited number of the more important constants. Fits using only primary force constants were tried first and then interaction constants were added later to achieve better agreement.

The optimum force field is given in Table 4 and the calculated frequencies it produces are listed in Table 5. The standard deviation is 10 cm^{-1} for 32 of the 36 allowed fundamentals.

The agreement between calculated and observed fundamental frequencies in the A_1 block is very good for both $Np(BH_4)_4$ and $Np(BD_4)_4$ while that in the others is satisfactory. As was noted in the analyses of the Zr and Hf analogs, the low energy modes do not agree as well as the higher frequency modes. This is particularly evident in $\nu_9^{T_2}$ and ν_5^E where the calculated E mode frequencies are lower than those of the corresponding T_2 modes in disagreement with experiment.

Since the derived force fields for $Zr(BH_4)_4$, $Hf(BH_4)_4$, and $Np(BH_4)_4$ are all slightly different in composition, one must be cautious in making close comparisons of the force constants. All primary force

constants follow the same trend and in the case of the νBH_t coordinates the values are nearly identical. All three fields give a large MB force constant and a very small MH_b constant indicating the possibility of significant MB bonding.

The allowed fundamentals which were not observed in the spectra were calculated at reasonable energies when compared to results from earlier work on the Zr and Hf compounds. In view of the fact that the A_1, E, and T_2 modes are calculated rather accurately, those values for the inactive T_1 modes should also be close to the correct energies. For example, the $\nu_4^{T_1}$ modes was observed for $Zr(BH_4)_4$ by inelastic neutron scattering[23] at 594 cm^{-1} and the corresponding 565 cm^{-1} value for that in $Np(BH_4)_4$ is quite reasonable. The overall trend found in this analysis even for the non T_2 modes is $\nu(Np) < \nu(Zr)$. Further assurance is given by the Teller-Redlich product rules for the T_1 symmetry block. The ratio for the calculated frequencies from Table 5 is 5.0 which is not in serious disagreement with the theoretical value of 6.4.

VI. Assignment of non-fundamental IR bands

A. 4000-200 cm^{-1} Region

The solid state IR spectra clearly show more bands than just fundamentals These extra features are either isotopic impurity, overtone, or combination bands. The impurity bands contain contributions from ^1H atoms in the borodeuteride molecules and ^{10}B atoms in both the borohydride and borodeuteride.

From gas phase IR spectra of the molecules $NpB_4H_xD_{16-x}$[24] prepared by intentionally reducing the time of reaction between $Np(BH_4)_4$ and D_2, the ^1H bands are easily assigned and are included in Tables 1 and 3. Similarly, bands are also seen in the Zr borodeuteride spectra.[13]

It is more difficult to locate ^{10}B modes since the isotopic shift is inherently smaller and there is always some of each isotope present in every sample. However frequency calculations of various isotopically substituted molecules, e.g. $Np(^{10}BH_4)_x(^{11}BH_4)_{4-x}$ and $Np(^{10}BD_4)_x(^{11}BD_4)_{4-x}$, using the force field in Table 4 were found to be very useful, in particular when $x=1$. The IR and Raman bands at 1931 cm^{-1}(D) and 1925 $\pm$ 5 cm^{-1}(D) mentioned in Section IV are nicely predicted by the calculations at 1931 cm^{-1} and contrary to previous explanations for analogous features in the spectra of $Zr(BD_4)_4$,[13] these bands are due to the ^{10}B isotope and not to a ^1H impurity. The great intensity of the 1931 cm^{-1} peak also substantiates this assignment. Similar ^{10}B effects are not observed for the borohydride since the change in reduced mass for a $^{10}B \rightarrow ^{11}B$ exchange in the borohydride is approximately half that in the borodeuteride.

In the $\nu BH_b(\nu BD_b)$ region, only $\nu_2^{T_2}$ is predicted to show a significant ^{10}B band and this is in agreement with the spectra. A separation of 11 cm^{-1} between $\nu_2^{T_2}$(D) and $^{10}B(\nu_2^{T_2}$(D)) is predicted and corresponds to a well resolved band at 1560 cm^{-1} as the ^{10}B mode.

Distinct ^{10}B effects are clearly visible in the $\nu M\dot{B}$ stretching region. Both the borohydride and borodeuteride fundamentals at 475 and 437 cm^{-1} reveal sub-bands of reasonable intensity but that in the borohydride spectrum at 509 cm^{-1} is too high in frequency to be $^{10}B(\nu_8^{T_2})$ with a $\nu^{10}/\nu^{11} > 1.050$. The 457 cm^{-1}(D) peak gives an acceptable frequency ratio of 1.046 and is assigned as $^{10}B(\nu_7^{T_2})$ but is predicted at only 444 cm^{-1}($x=1$) and 449 cm^{-1}($x=4$). For a more detailed understanding of ^{10}B effects in the vibrational spectra, isotopically pure samples would have to be examined experimentally.

An interesting non-fundamental band is the $\sim$1600 cm^{-1} features in both

the gas and solid state IR spectra and Raman spectrum of $Np(BD_4)_4$.
It is apparent from Table 5 that while the agreement between the ob-
served and calculated frequencies for $\nu_2^{T_2}(H)$ is very good, that for the
borodeuteride is surprisingly poor. The fact that the 1593 cm^{-1}(D) is
so intense for a non-fundamental transition and that $\nu_2^{T_2}(D)$ is so far
removed from its calculated position suggests that Fermi resonance is
important. Identical effects in this same energy region are also observed
for $Zr(BH_4)_4$,[13,20] $Hf(BD_4)_4$,[9,14] $U(BD_4)_4$,[12] and $Al(BD_4)_3$.[19] A possible
explanation was given for the $Zr(BD_4)_4$ case as the overtone of a very weak,
unassigned feature at 812 cm^{-1} in Fermi resonance with $\nu_2^{T_2}(D)$ at 1603 cm^{-1}.
Later, the third band was assigned as $\nu_1^{T_1}$ in an analysis which assumed the
T symmetry model for $Zr(BD_4)_4$.[13]

In choosing overtones that could be in resonance with a T_2 species,
only T_1 and T_2 modes can be considered. In this work, the 1593 cm^{-1}(D)
band is tentatively assigned as the T_2 component of $2\nu_3^{T_1}$ (of symmetry
species $A_1 + E + T_2$) in resonance with $\nu_2^{T_2}$ causing the observed perturba-
tion of energies and intensities. From an inspection of Table 5, the most
likely fundamental to give an overtone near 1600 cm^{-1} is $\nu_3^{T_1}$ even though
only the calculated value is available. Other possible states which could
interact with $\nu_2^{T_2}$ are the combination levels containing a T_2 species but
any firm assignment of such a level must await further data.

The νBD_b fundamentals of $Np(BD_4)_4$, $\nu_2^{T_2}$ and $\nu_3^{T_2}$, were seen to give
relatively strong overtones at 3012 and 3074 cm^{-1}, respectively. Also the
δHBH bending region in the borohydride (1100-1200 cm^{-1}) exhibits overtones
in the solid state IR spectrum.

B. 7400-4000 cm^{-1} Region

The near IR spectra of Zr and Np borohydrides are shown in Fig. 6 and listings of the observed bands and their assignments are given in Tables 6 and 7.

Overtones of the νBH_t modes are seen at the high energy end of the spectra in Fig. 6 with the weaker ^{10}B modes clearly visible. From the spectrum of a 1 mm thick $Zr(BH_4)_4$ crystal, the 2nd overtone of the $\nu_1^{T_2}$ fundamental was observed. Similar overtones of $\nu_1^{T_2}(D)$ of $Np(BD_4)_4$ were not visible in the IR spectrum (Fig. 2) apparently because they were buried in the broad absorption due to surface moisture on the CsI windows seen in the region 4000-3700 cm^{-1}.

The next group of bands are those in the 2100-2250 nm (4750-4450 cm^{-1}) region. From Table 5 it appears that no first or second overtone of any T_1 or T_2 fundamental has the correct energy. Although third overtones of the 1200 cm^{-1} region are reasonable assignments from energy considerations, they are not expected to be as intense as are the observed bands since the second overtones do not occur near 3400 cm^{-1}. Similar reasoning also rejects the assignments $4\nu_6^{T_2}$ and $4\nu_3^{T_1}$. The only possible origins left are combination bands and possible ones are given in Tables 6 and 7.

The last group of bands are the most intense ones between 2350 and 2470 nm (4250-4050 cm^{-1}). The three bands in each spectrum are due to overtones of the three νBH_b stretching modes $(2T_2, 1T_1)$ in the energy range 2150-2060 cm^{-1} for $Np(BH_4)_4$ and 2180-2100 cm^{-1} for $Zr(BH_4)_4$. In contrast to the borohydride spectra which show 3 distinct bands, the borodeuteride spectra (see Fig. 2 of this work and Table 3, ref. 13) show only 2 bands in which the effects of Fermi resonance has possibly caused the overlap of $2\nu_2^{T_2}$ and $2\nu_1^{T_1}$.

Based on the frequencies for $\nu_2{}^{T_2}$, $\nu_3{}^{T_2}$ and $\nu_1{}^{T_1}$ calculated for $Np(BH_4)_4$, the observed bands at 4064, 4126, and 4169 cm^{-1} are assigned as $2\nu_3{}^{T_2}$, $2\nu_1{}^{T_1}$, and $2\nu_2{}^{T_2}$, respectively. Although the intensity of the 4113 cm^{-1} band might favor its assignment as $2\nu_1{}^{T_1}$, this would suggest that the 4126 cm^{-1} peak is due to ^{10}B modes. The latter absorption band is too intense for a ^{10}B mode since at least two ^{10}B atoms per molecule are needed to produce the 13 cm^{-1} shift and those molecules are only 15.4% abundant.[20] Therefore the 4113 cm^{-1} band is assigned as $2\nu_{2a}{}^{T_2}$ which appears as a sharp, medium intensity absorption in the $Np(BH_4)_4$ spectrum at 2110 cm^{-1}. The overtone of the ^{10}B mode is calculated to be about 10-12 cm^{-1} higher than that of ^{11}B for $2\nu_2{}^{T_2}$ and this agrees well with the 4180 cm^{-1} shoulder both in terms of energy and intensity.

The overtones in the 4250-4050 cm^{-1} region for $Zr(BH_4)_4$ are not as well resolved but three bands are discernible. By analogy with the previous assignment for $Np(BH_4)_4$, the bands at 4153, 4174, and 4230 cm^{-1} are assigned as $2\nu_3{}^{T_2}$, $2\nu_1{}^{T_1}$, and $2\nu_2{}^{T_2}$, respectively. This conforms to the assignments made in the $Zr(BH_4)_4$[13] and $Hf(BH_4)_4$[14] studies which used the T_d model.

The near IR spectrum of $Zr(BD_4)_4$ is shown in Fig. 7 and a listing of the observed bands is given in Table 8. The very low intensities of the bands is the result of the fact that high order overtone and combinations observed are due to the fundamentals occurring at relatively low energy. This also increases the number of possible choices for assignments of the bands to the point where no firm decisions can be drawn from the present spectra.

No overtone of $\nu_1^{T_2}$ (D) is predicted anywhere in the areas where bands are seen. The second overtone of $\nu_3^{T_2}$ is probably the 4545 cm^{-1} band showing small ^{10}B effects as a high-frequency shoulder. The remaining bands were assigned as combinations which were allowed and had a calculated energy in reasonable agreement with those observed.

VII. Entropy and Heat Capacity

The entropy and heat capacity for $Np(BH_4)_4$ were calculated from the partition function, $Q = Q_t Q_r Q_v$, using the methods of statistical thermodynamics.[25] The vibrational partition function, Q_v, was determined from the fundamental frequencies given in Table 5. Both free[26] and hindered[25] internal rotation were considered in the calculation of Q_r where the BH_4 groups rotate about the M-B axes. The barrier potential energy was assumed to have the form $V = 1/2\ V_0(1-cos3\phi)$, where the value $V_0 = 3420$ cal/mol found for $Zr(BH_4)_4$[23] was used for $Np(BH_4)_4$. The value of V_0 for $Np(BH_4)_4$ is unknown and is most likely different than that for $Zr(BH_4)_4$ but a 50% deviation in V_0 would cause less than a 5% error in the entropy and heat capacity. Table 9 gives the total sums of all contributions and these are compared to experimental and calculated values for $Hf(BH_4)_4$[27] and the structurally related compounds $Pb(CH_3)_4$,[28] $Sn(CH_3)_4$,[29] $Ge(CH_3)_4$,[29] $Si(CH_3)_4$,[29,30] and $C(CH_3)_4$.[31] It can be seen that although the $M(CH_3)_4$ molecules have slightly fewer atoms giving lower heat capacities and entropies, the thermodynamic quantities are comparable. From the partition functions, the greatest deviation occurs in the vibrational contribution.

VIII. Conclusion

Although the solid state structure of $Np(BH_4)_4$ is slightly different
than that of Zr and Hf borohydrides, their basic similarities are clearly
reflected in the vibrational spectra. There are a few differences, however,
seen mostly in the lower energy region in the solid state spectra, which
also persist in the gas phase where all $M(BH_4)_4$ molecules are isostructural.

The 2600-2400 cm^{-1} (2000-1800 cm^{-1}) region shows the same pattern for
Np, Zr and Hf borohydrides--the sharp $\nu BH_t(\nu BD_t)$ fundamental and a broad
set of overtones due to modes in the 1200 cm^{-1} (900 cm^{-1}) range. The
$\nu BH_b(\nu BD_b)$ bands in the 2150-2000 cm^{-1} (1600-1500 cm^{-1}) region are also
very similar in appearance even for the borodeuterides where Fermi resonance
is observed for all those compounds. A close resemblance is also noted
in the near IR spectra of $Np(BH_4)_4$ and $Zr(BH_4)_4$ (Fig. 6) which are comprised
of overtone transitions of the νBH_t and νBH_b modes.

Slight differences of several types are observed in the
remaining spectral regions for the Np and Zr, Hf compounds. The
νMH_b, δHBH (νMD_b, δDBD) modes seen in the 1250-1050 cm^{-1} (950-800 cm^{-1})
range are very dependent on the size of the $MH_3B(MD_3B)$ cage and mass of
the metal atom as determined by the normal coordinate calculations using
various size cages and metal masses. Smaller cages and lighter metals
produce higher frequency normal modes. Frequencies were also found to
be very dependent on the positions of the H_b atoms in the coordination
sphere of the metal. Therefore the ν_4^{T2}, ν_5^{T2}, and ν_6^{T2} modes for the
actinide compounds, whose masses and sizes are very similar, are more alike
among themselves than they are to those of the lighter and smaller Zr and Hf
analogs.

The νMB region, unlike the 1600-1500 cm^{-1} region in the borodeuteride spectra, shows Fermi resonance only for the lighter $Zr(BD_4)_4$ and $Hf(BD_4)_4$ giving significant intensity to $\nu_8{}^{T_2}(D)$. Since the stretching modes in the 500-400 cm^{-1} region are not highly sensitive to size effects, metal mass differences are therefore primarily responsible for governing the extent of resonance between $\nu_7{}^{T_2}(D)$ and $\nu_8{}^{T_2}(D)$. Due to the large separation of $\nu_7{}^{T_2}(H)$ and $\nu_8{}^{T_2}(H)$, mass effects are inadequate to induce resonance and the spectra are basically the same for all compounds except that the modes for the heavier molecules occur at lower energies.

The lowest frequency vibrations, $\nu_9{}^{T_2}$ and $\nu_5{}^{E}$, are mainly δHMH bends where the former involves the greatest amount of metal motion of all modes. Consequently it gives the largest frequency shift for a given change in metal mass and is observed ~ 70 cm^{-1} lower in $Np(BH_4)_4$ than in the Zr compound. The large shift of $\nu_5{}^{E}$, also about 70 cm^{-1}, indicates that other effects such as H_b - H_b interactions and M - H_b bond strengths must be important.

Although the two force fields found for $Np(BH_4)_4$ and $Hf(BH_4)_4$[14] cannot be compared in fine detail, the values of the force constants are very similar especially those related to the BH_4 group. This is to be expected since it was observed that the BH_4 modes are not strongly dependent on metal size or mass. Greater differences are found in the force constants involving the MH_3B structures but in general follow the same trend where the MB constant is higher than the MH_b constant. As was also noted in the vibrational analyses of Hf and Zr borohydrides, MB bonding may be significant in these molecules.

Acknowledgment

Appendix

In this paper a fundamental or overtone is denoted by the symbol $n\nu_a^b$, where b is the Mulliken symbol for the irreducible representation of the mode and a is the number of the mode starting with 1 for the highest frequency, 2 for the second highest, etc. The n is omitted for fundamentals, equals 2 for first overtones, 3 for second overtones, etc.

The table given below relates our notation to that used in earlier work ($\underline{7b}$,15).

This work	Literature
$\nu_1^{A_1} - \nu_4^{A_1}$	$\nu_1 - \nu_4$
ν^{A_2}	ν_5
$\nu_1^{E} - \nu_5^{E}$	$\nu_6 - \nu_{10}$
$\nu_1^{T_1} - \nu_5^{T_1}$	$\nu_{11} - \nu_{15}$
$\nu_1^{T_2} - \nu_9^{T_2}$	$\nu_{16} - \nu_{24}$

References

1. Schlesinger, H.I.; Brown, H.C. J. Am. Chem. Soc. 1953, 75, 219.

2. Hoekstra, H.R.; Katz, J.J. J. Am. Chem. Soc. 1949, 71, 2488.

3. Banks, R.H.; Edelstein, N.M.; Rietz, R.R.; Templeton, D.H.; Zalkin, A. J. Am. Chem. Soc. 1978, 100, 1957.

4. James, B.D.; Smith, B.E.; Wallbridge, M.G.H. J. Mol. Struct. 1972, 14, 327.

5. Ghiassee, N.; Clay, P.G.; Walton, G.N. Inorg. Nucl. Chem. Lett. 1978, 14, 117.

6. Banks, R.H.; Edelstein, N.M.; Spencer, B.; Templeton, D.H.; Zalkin, A. J. Am. Chem. Soc. 1980, 102, 620.

7a. Bernstein, E.R.; Hamilton, W.C.; Keiderling, T.A.; LaPlaca, S.J.; Lippard, S.J.; Mayerle, J.J. Inorg. Chem. 1972, 11, 3009.

7b. Bernstein, E.R.; Keiderling, T.A.; Lippard, S.J.; Mayerle, J.J. J. Am. Chem. Soc. 1972, 94, 2552.

8. Bird, P.H.; Churchill, M.R. Chem. Comm. 1967, 403.

9. Keiderling, T.A. Ph. D. Thesis, Princeton University, 1974.

10. Volkov, V.V.; Myakishev, K.G.; Grankina, Z.A. Russ. J. Inorg. Chem. 1970, 15, 1490.

11. Banks, R.H. Ph.D. Thesis, University of California, 1979.

12. Paine, R.T.; Light, R.W.; Nelson, M. Spectrochim. Acta. 1979, 35A, 213.

13. Smith, B.E.; Shurvell, H.F.; James, B.D. J. Chem. Soc. Dalton 1978, 710.

14. Keiderling, T.A.; Wozniak, W.T.; Gay, R.S.; Jurkowitz, D.; Bernstein, E.R.; Lippard, S.J.; Spiro, T.G. Inorg. Chem. 1975, 14, 576.

15. Bernstein, E.R.; Keiderling, T.A. J. Chem. Phys. 1973, 59, 2105.

16. Joyce, R.R.; Richards, P.L. Phys. Rev. 1969, 179, 375.

17. Broach, R.S.; Chuang, I.S.; Williams, J.M.; Marks, T.J. Private communication, 1979.

18. Herzberg, G. "Infrared and Raman Spectra" D. Van Nostrand Co. Inc., Princeton, N.J. 1945.

19. Coe, D.A.; Nibler, J.W. Spectrochim. Acta. 1973, 29A, 1789.

20. Davies, N.; Wallbridge, M.G.H.; Smith, B.E.; James, B.D. J. Chem. Soc. Dalton 1973, 162.

21. Gwinn, W.D. J. Chem. Phys. 1971, 55, 477.

22. Reuter, D.; Gwinn, W.D. To be submitted to QCPE.

23. Tomkinson, J.; Waddington, T.C. J. Chem. Soc. Faraday II. 1976, 1245.

24. Unpublished results in our laboratory, 1978.

25. Pitzer, K.S.; Brewer, L. "Thermodynamics" McGraw-Hill Book Co. New York, 1961.

26. Pitzer, K.S.; Gwinn, W.D. J. Chem. Phys. 1942, 10, 428.

27. The fundamental frequencies and molecular structure parameters used in the thermodynamic calculations were taken from Ref. 14.

28a. Crowder, G.A.; Gorin, G.; Kruse, F.H.; Scott, D.W. J. Mol. Spect. 1965, 16, 115.

28b. Good, W.D.; Scott, D.W.; Lacina, J.L.; McCullough, J.P. J. Phys. Chem. 1959, 63, 1139.

29. Lippincott, E.R.; Tobin, M.C. J. Am. Chem. Soc. 1953, 75, 4141.

30a. Shimizu, K.; Murata, H. J. Mol. Spect. 1960, 5, 44.

30b. Aston, J.G.; Kennedy, R.M.; Messerly, G.H. J. Am. Chem. Soc. 1941, 63, 2343.

31a. Pitzer, K.S. J. Chem. Phys. 1937, 5, 473.

31b. Aston, J.G.; Messerly, G.H. J. Am. Chem. Soc. 1936, 58, 2354.

Table 1

Observed Bands in Gas Phase IR Spectra of $Np(BH_4)_4$ and $Np(BD_4)_4$

Energy (cm^{-1})	Assignment	Internal Coordinates	Comments
	$Np(BH_4)_4$		
2568	$\nu_1^{T_2}$	νBH_t	strong
2480	$2\nu_4^{T_2}, \ 2\nu_5^{T_2}$		weak, v. broad
2350	$\nu_{4,5}^{T_2} + \nu_6^{T_2}$		weak, broad
2155	$\nu_2^{T_2}$	νBH_b	strong
2130	$\nu_{2a}^{T_2}a$		shoulder on $\nu_2^{T_2}$
2084	$\nu_3^{T_2}$	νBH_b	strong, sharp
1280			shoulder on $\nu_{4,5}^{T_2}$
1240	$\nu_4^{T_2}, \ \nu_5^{T_2}$	$\delta HBH, \ \nu MH_b$	v. strong, broad
1205	$\nu_3^{E} + \nu_9^{T_2}$		shoulder on $\nu_{4,5}^{T_2}$
1122	$\nu_6^{T_2}$	δHBH	medium, broad
1080			shoulder on $\nu_6^{T_2}$
478	$\nu_8^{T_2}$	$\nu MB, \ \nu MH_b$	strong
	$Np(BD_4)_4$		
3092	$2\nu_2^{T_2}$		v. weak, broad
3030	$2\nu_3^{T_2}$		v. weak, broad
1930	$^{10}B(\nu_1^{T_2})b$	$\nu^{10}BD_t$	shoulder on $\nu_1^{T_2}$
1922	$\nu_1^{T_2}$	νBD_t	strong
1605	$2\nu_3^{T_1}c$		medium
1562	$^{10}B(\nu_2^{T_2})$	$\nu^{10}BD_b$	shoulder on $\nu_2^{T_2}$
1558	$\nu_2^{T_2}c$	νBD_b	strong
1526	$\nu_3^{T_2}$	νBD_b	strong, sharp
1190	^1H	δHBD	weak, broad
928	$\nu_{4,5}^{T_2}$	$\delta DBD, \ \nu MD_b$	v. strong
845	$\nu_6^{T_2}$	δDBD	weak, broad

Table 1 (continued)

Energy (cm^{-1})	Assignment	Internal Coordinates	Comments
		$Np(BD_4)_4$	
810			shoulder on $\nu_6^{T_2}$
437	$\nu_7^{T_2}$	$\nu MB, \nu MD_b$	strong

In the table: H_t = terminal hydrogen, H_b = bridging hydrogen, ν = very

[a] This feature could not be assigned with any certainty so it was given the identifying symbol, $\nu_{2a}^{T_2}$.

[b] A fundamental in parenthesis next to an impurity atom is that mode in which the impurity atom is participating.

[c] These two bands are in Fermi resonance.

Table 2

Observed Bands in 77K IR (4000–25 cm^{-1}) and Raman (2600–100 cm^{-1})

Spectra of $Np(BH_4)_4$

Energy (cm^{-1})	Assignment	Internal Coordinates	Comments
2557	$\nu_1{}^{A_1}$	νBH_t	medium, R.
2551	$\nu_1{}^{T_2}$	νBH_t	strong, sharp, IR
2490	$2\nu_4{}^{T_2}$		weak, IR
2445	$2\nu_5{}^{T_2}$		weak, IR
2378	$\nu_4{}^{T_2} + \nu_6{}^{T_2}$		weak, broad, IR
2149	$\nu_2{}^{A_1}$	νBH_b	medium, R
2143	$\nu_2{}^{T_2}$	νBH_b	strong, sharp, IR
2123	$\nu_1{}^{E}$	νBH_b	medium, R
2117	$^{10}B(\nu_{2a}{}^{T_2})$		medium, shoulder
2110	$\nu_{2a}{}^{T_2}$		medium, sharp, IR
2069 (2070)^a			strong, sharp doublet
2059 (2060)	$\nu_3{}^{T_2}$	νBH_b	medium, + shoulder, R
1283	$\nu_3{}^{A_1}$	νMH_b, δHBH^b	medium, R
1276			medium, sharp, IR
1260	$\nu_2{}^{E}$	νMH_b, δHBH	weak, R
1247 (1255)	$\nu_4{}^{T_2}$	νMH_b, δHBH	v. strong IR, medium, R
1225 (1230)	$\nu_5{}^{T_2}$	νMH_b, δHBH	v. strong IR, medium, R
1199 (1205)	$\nu_3{}^{E} + \nu_9{}^{T_2}$		medium IR, weak, R
1159			medium +, IR
1138 (1127)	$\nu_6{}^{T_2}$	δHBH, νMH_b	strong, IR, weak, R
1068			weak, IR
1053	$\nu_3{}^{E}$	δHBH	medium, R
639	$\nu_8{}^{T_2} + \nu_5{}^{E}$		weak, R
611	$\nu_8{}^{T_2} + \nu_9{}^{T_2}$		weak, IR
517	$\nu_4{}^{A_1}$	νMB	strong, R
509 (506)			weak, sharp, IR, medium, R

Table 2 (continued)

Energy (cm^{-1})	Assignment	Internal Coordinates	Comments
475 (~480)	$\nu_8^{T_2}$	νMB	v. strong, IR, shoulder, R
168	ν_5^{E}	δHMH	v. strong, sharp, R
130 (141)	$\nu_9^{T_2}$	δHMH	strong, IR, medium R

[a] T_2 modes also seen in the Raman are shown next to the IR value in parenthesis.

[b] The more important internal coordinates are to the left of the lesser important ones.

Table 3

Observed Bands in 77K IR (4000-25 cm^{-1}) and Raman (2300-100 cm^{-1})

Spectra of Np(BD$_4$)$_4$

Energy (cm^{-1})	Assignment	Internal Coordinates	Comments
3092	$^{10}B(2\nu_2{}^{T_2})$		v. weak, IR
3074	$2\nu_2{}^{T_2}$		weak, sharp, IR
3012	$2\nu_3{}^{T_2}$		weak, sharp, IR
2110	$^1H(\nu_3{}^{T_2}(H))$	νBH_b	weak, IR
1979			weak, broad, IR
1931	$^{10}B(\nu_1{}^{T_2})$	$\nu^{10}BD_t$	medium, sharp, IR
1925	$^{10}B(\nu_1{}^{A_1})$	$\nu^{10}BD_t$	shoulder, R
1913	$\nu_1{}^{A_1}$	νBD_t	medium +, R
1912	$\nu_1{}^{T_2}$	νBD_t	strong, sharp, IR
1842	$2\nu_4{}^{T_2}$		weak, sl. broad, IR
~1780 (~1780)	$\nu_4{}^{T_2} + \nu_6{}^{T_2}$		weak, v. broad, IR, R
1619	$\nu_1{}^{E}$	νBD_b	weak, R
1621, 1614, 1604, 1598	$^{10}B,\ ^1H(2\nu_3{}^{T_1})?$		medium, sharp, IR
1593 (1592)	$T_2(2\nu_3{}^{T_1})^a$		medium +, sharp, IR, R
1560	$^{10}B(\nu_2{}^{T_2})$	$\nu^{10}BD_b$	medium, sharp, IR
1548 (1549)	$\nu_2{}^{T_2}{}^a$	νBD_b	strong, sharp IR, medium R
1517	$\nu_2{}^{A_1}$	νBD_b	strong, sharp, R
1516	$\nu_3{}^{T_2}$	νBD_b	v. strong, sharp, IR
1251	$^1H(\nu_4{}^{T_2}(H))$	νMH_b, δHBD	weak, v. broad, IR
1191	$^1H(\nu_{4,5}{}^{T_2}(H))$	νMH_b, δHBD	weak +, sharp, IR
955	$\nu_3{}^{A_1}$	νMD_b, δDBD	weak +, R
941			strong, sharp, IR
926	$\nu_4{}^{T_2}$	νMD_b, δDBD	strong, IR
917	$\nu_5{}^{T_2}$	νMD_b, δDBD	strong, IR
910	$\nu_3{}^{E} + \nu_9{}^{T_2}$		strong, IR

Table 3 (continued)

Energy (cm^{-1})	Assignment	Internal Coordinates	Comments
905	ν_2^E	δDBD, νMD_b	weak, sl. broad, R
860 (863)	$\nu_6^{T_2}$	δDBD	strong, sharp, IR, weak, R
838			weak, IR
802			weak, IR
795	ν_3^E	δDBD	weak, R
475	$\nu_4^{A_1}$	νMB	strong, R
457	$^{10}B(\nu_7^{T_2})$	$\nu M^{10}B$	medium, sharp IR
437 (440)	$\nu_7^{T_2}$	νMB	v. strong, IR, shoulder, R
406			v. weak, IR
154	ν_5^E	δDMD	v. strong, sharp, R
112 (121)	$\nu_9^{T_2}$	δDMD	strong, IR, medium, R

[a]These two bands are in Fermi resonance.

Table 4

Best-Fit Force Constants for Neptunium Borohydride at 77K

Primary Force Constants		Interaction Force Constants	
Internal Coordinates	Value	Internal Coordinates	Value
νBH_t	3.51 md/Å	$\nu BH_b : \nu BH_b^{\,b}$	.04 md/Å
νBH_b	2.36	$\nu MH_b : \nu MH_b$	.02
νMH_b	.37	$\nu MB : \delta H_b MH_b$	−.09 md
νMB	1.28	$\nu BH_b : \delta H_b BH_b^{\,b}$	.04
$\delta H_t BH_b$	.28 mdÅ	$\nu MH_b : \delta H_b MH_b$	.04
$\delta H_b BH_b$	.36		
$\delta H_b MH_b \ (C_3)$	.26		
$\epsilon H_b BMB$	.18[a]		

[a]·The torsion force constant is essentially undetermined since the A_2 mode is not observed. It was set at .18 and kept constant during all fits.

[b]·Internal coordinates in this constant interact only with other like coordinates in the same BH_4 group.

Table 5

Fundamental Vibrations (cm^{-1}) of $Np(BH_4)_4$ and $Np(BD_4)_4$

Normal Mode	$Np(BH_4)_4$		$Np(BD_4)_4$	
	Observed	Calculated	Observed	Calculated
$\nu_1^{T_2}$	2551	2557	1912	1911
$\nu_2^{T_2}$	2143	2144	1548[a]	1603
$\nu_3^{T_2}$	2069	2078	1516	1485
$\nu_4^{T_2}$	1247	1266	926	897
$\nu_5^{T_2}$	1225	1223	917	895
$\nu_6^{T_2}$	1138	1104	860	824
$\nu_7^{T_2}$	————	575	437	447
$\nu_8^{T_2}$	475	488	————	415
$\nu_9^{T_2}$	130	156	112	139
$\nu_1^{A_1}$	2557	2554	1913	1905
$\nu_2^{A_1}$	2149	2147	1517	1523
$\nu_3^{A_1}$	1283	1284	955	953
$\nu_4^{A_1}$	517	517	475	466
ν_1^{E}	2123	2117	1619	1589
ν_2^{E}	1260	1270	905	899
ν_3^{E}	1053	1089	795	807
ν_4^{E}	————	571	————	413
ν_5^{E}	168	142	154	125
$\nu_1^{T_1}$	————	2116	————	1587
$\nu_2^{T_1}$	————	1256	————	889
$\nu_3^{T_1}$	————	1084	————	810
$\nu_4^{T_1}$	————	565	————	405
$\nu_5^{T_1}$	————	405	————	288
ν^{A_2}	————	288	————	204

[a]This mode is in Fermi resonance with $2\nu_3^{T_1}(D)$.

Table 6

Observed IR Bands $(7400\text{-}4000\ cm^{-1})$ of $Np(BH_4)_4$ at 2K

Wavelength (nm)	Energy (cm^{-1})	Assignment	Comments
2460	4064	$2\nu_3^{T_2}$	v. strong
2457	4070	$^{10}B(2\nu_3^{T_2})$?	shoulder on $2\nu_3^{T_2}$
2447	4086	$\nu_2^{T_2} + \nu_3^{T_2}$	weak shoulder
2431	4113	$2\nu_{2a}^{T_2}$*	strong, sharp
2423	4126	$2\nu_1^{T_1}$	medium, sharp
2398	4169	$2\nu_2^{T_2}$	medium, sharp
2392	4180	$^{10}B(2\nu_2^{T_2})$	shoulder on $2\nu_2^{T_2}$
2378	4205	$\nu_3^{T_2} + \nu_6^{T_2} + \nu_3^{E}$	broad, v. weak
2335	4281	$2\nu_6^{T_2} + \nu_3^{T_2}$	broad, weak
2237	4469	$\nu_1^{T_2} + 2\nu_3^{T_2}$	v. broad, v. weak
2201	4542	$\nu_3^{T_2} + 2\nu_4^{T_2}$	broad, weak +
2165	4618	$\nu_2^{T_2} + 2\nu_4^{T_2}$	broad, weak
2129	4696	$\nu_2^{T_2} + 2\nu_3^{A_1}$	broad, weak
1994	5013	$2\nu_1^{T_2}$	weak, sharp
1986	5033	$^{10}B(2\nu_1^{T_2})$	weak
1654	6046	$3\nu_3^{T_2}$	broad
1353	7389	$3\nu_1^{T_2}$	weak

*See Table 1, footnote a.

Table 7

Observed IR Bands (7500–4000 cm^{-1}) of $Zr(BH_4)_4$ at 2K

Wavelength (nm)	Energy (cm^{-1})	Assignment	Comments
2407	4153	$2\nu_3^{T_2}$	shoulder, intense
2395	4174	$2\nu_1^{T_1}$ a	strong
2363	4230	$2\nu_2^{T_2}$	medium, broad
2290	4366	$\nu_3^{T_2} + \nu_6^{T_2} + \nu_3^{E}$	v. weak, broad
2261	4422	$\nu_3^{T_2} + 2\nu_6^{T_2}$	v. weak, broad
1976	5058	$2\nu_1^{T_2}$	weak +, sharp
1968	5080	$^{10}B(2\nu_1^{T_2})$	weak
1946 b	5138		medium
1634	6117	$3\nu_3^{T_2}$	v. intense, sharp
1621	6167	$3\nu_1^{T_1}$	shoulder on 3 ^{T}
1592	6279	$3\nu_2^{T_2}$	weak
1579	6332		medium, broad
1341	7458	$3\nu_1^{T_2}$	medium, sharp
1335	7487	$^{10}B(3\nu_1^{T_2})$	weak

a The calculated value for $\nu_1^{T_1}$ was taken from Ref. 14 for $Hf(BH_4)_4$.

b This band and the others listed below it are taken from the spectrum of the 1 mm pathlength crystal.

Table 8

Observed IR Bands (4800–4000 cm^{-1}) of $Zr(BD_4)_4$ at 2K

Wavelength (nm)	Energy (cm^{-1})	Assignment	Comments
2455	4072	$\nu_2^{T_2} + 3\nu_6^{T_2}$	medium
2394	4176	$\nu_3^{T_2} + 2\nu_5^{T_2} + \nu_6^{T_2}$	strong
2347	4259	$\nu_2^{A_1} + 3\nu_5^{T_2}$	strong
2238	4486	$\nu_1^{T_2} + 2\nu_6^{T_2} + \nu_5^{T_2}$	weak +, broad
2199	4545	$3\nu_3^{T_2}$	strong
2175	4597	$\nu_2^{A_1} + 2\nu_3^{T_2}$	strong
2165	4617	$2\nu_2^{A_1} + \nu_3^{T_2}$	weak +
2148	4655	$3\nu_2^{T_2}$	weak

Table 9

Entropies and Heat Capacities of $Hf(BH_4)_4$, $Np(BH_4)_4$ and $M(CH_3)_4$

Heat Capacities [a]

$Hf(BH_4)_4$		$Np(BH_4)_4$		$Pb(CH_3)_4$	$Sn(CH_3)_4$	$Ge(CH_3)_4$	$Si(CH_3)_4$	$C(CH_3)_4$
FIR	HIR	FIR	HIR	FIR	FIR	FIR	FIR	
45.09	49.77	45.93	50.52	34.42	33.34	31.98	33.39	-------

Entropies

$Hf(BH_4)_4$		$Np(BH_4)_4$		$Pb(CH_3)_4$	$Sn(CH_3)_4$	$Ge(CH_3)_4$	$Si(CH_3)_4$	$C(CH_3)_4$
FIR	HIR	FIR	HIR	FIR	FIR	FIR	FIR	FIR
102.51	96.04	107.30	100.76	100.5	96.11	91.99	88.25	80.12
				100.48 [b]			86.04 [b]	71.71 [c]

In the table: FIR = free internal rotation, HIR = hindered internal rotation. All values for C_p^o and S^o are for the ideal gas at 298.15K and are in units of cal/deg.

[a] All C_p^o values are calculated.

[b] Experimental values.

[c] Experimental value at 282.6K. Ref. 31(b).

Figure Captions

Figure 1.   Gas Phase IR Spectra of $Np(BH_4)_4$ and $Np(BD_4)_4$.

Figure 2.   Solid-State IR Spectra of $Np(BH_4)_4$ and $Np(BD_4)_4$ at 77K.

Figure 3.   Far IR Spectrum of $Np(BH_4)_4$ at 77K.

Figure 4.   Raman Spectrum of $Np(BH_4)_4$ at 77K.

Figure 5.   Raman Spectrum of $Np(BD_4)_4$ at 77K.

Figure 6.   Near IR Spectra of $Np(BH_4)_4$ and $Zr(BH_4)_4$ at 2K.

Figure 7.   Near IR Spectrum of $Zr(BD_4)_4$ at 2K.
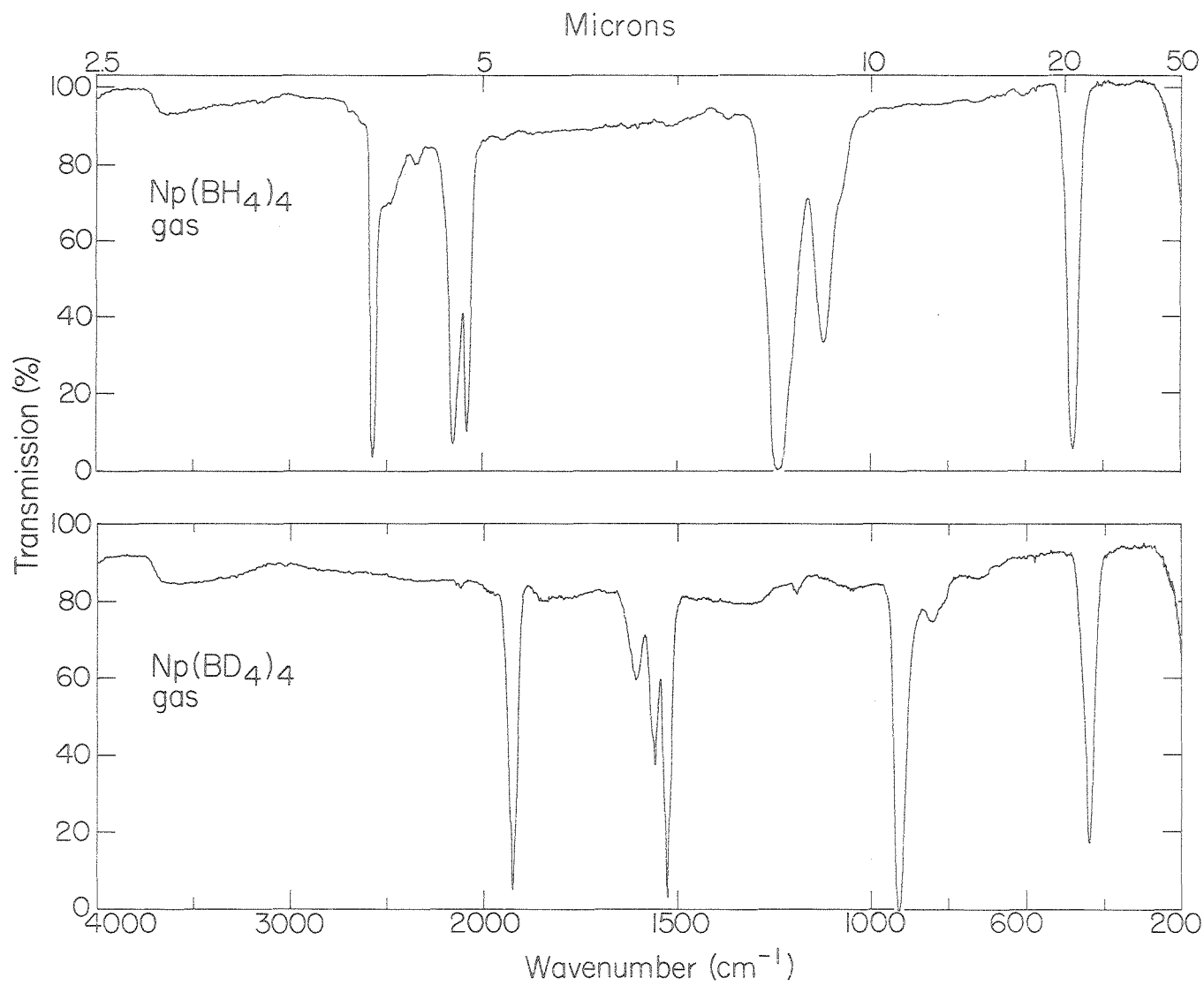
Figure 1.

XBL798-2702
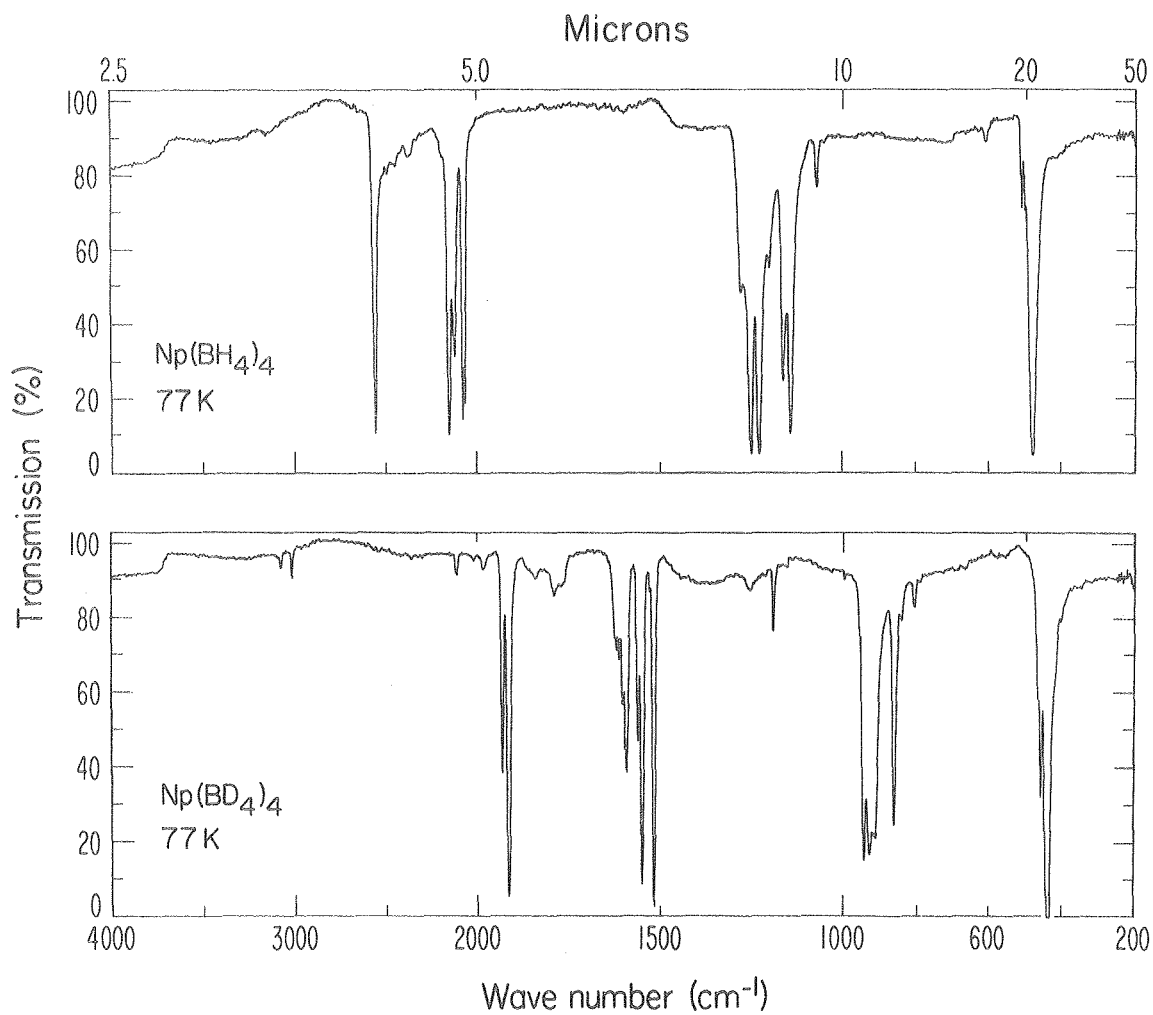
Figure 2.
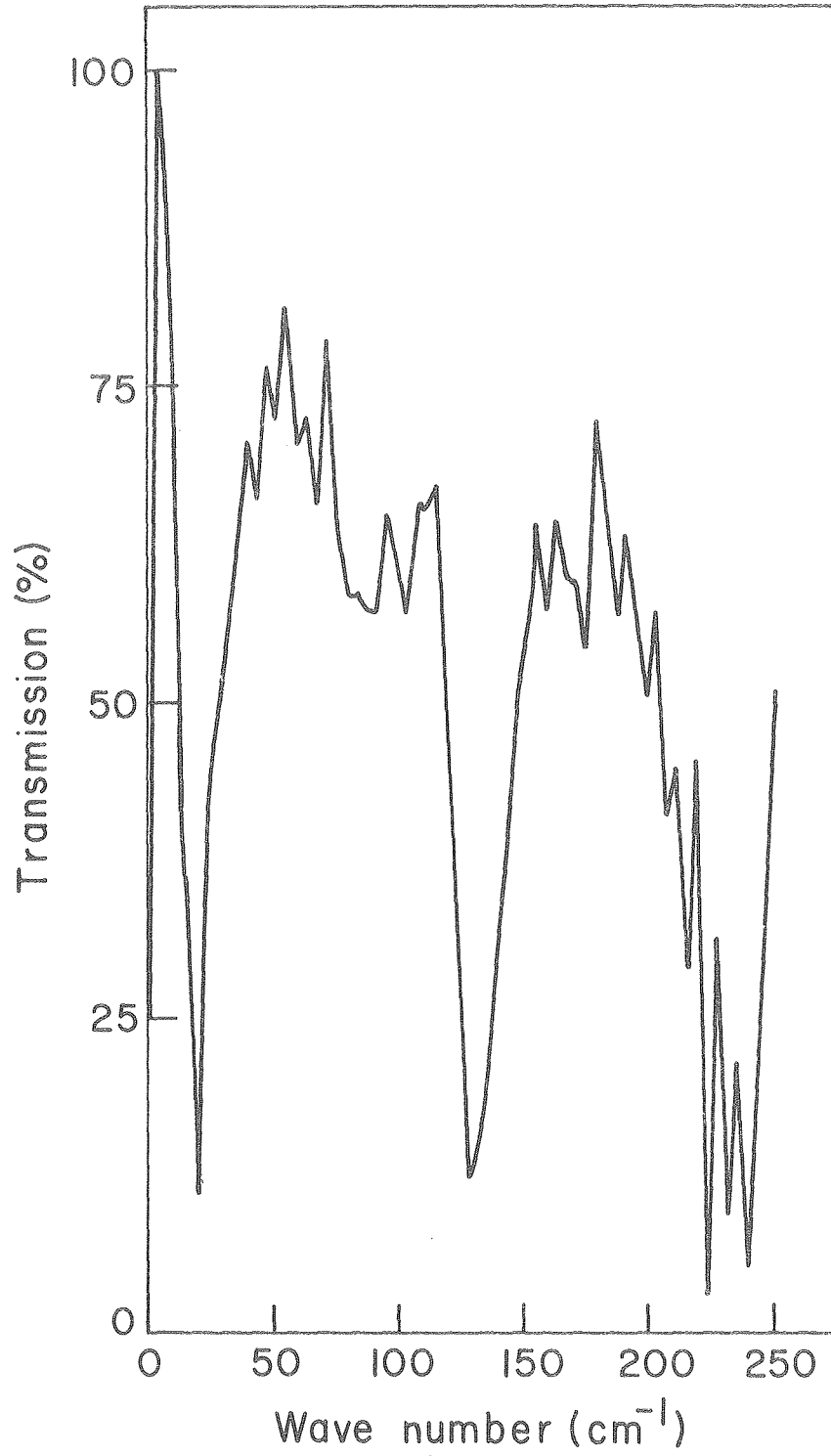
Figure 3.

XBL 796-1919

42.

$Np(BH_4)_4$
77K
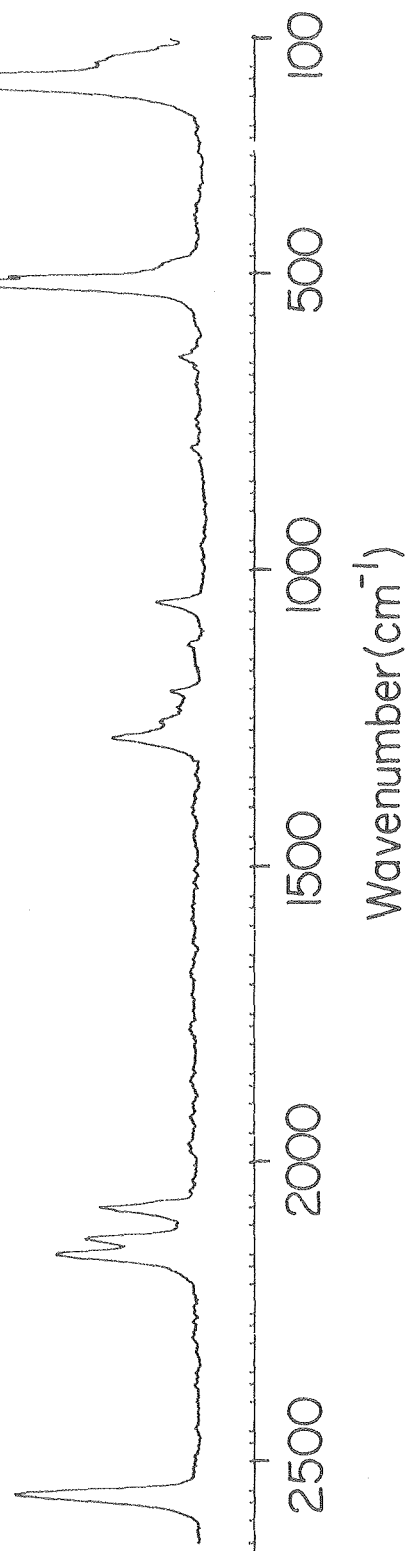
Wavenumber(cm^{-1})

Figure 4.

XBL 796-1878
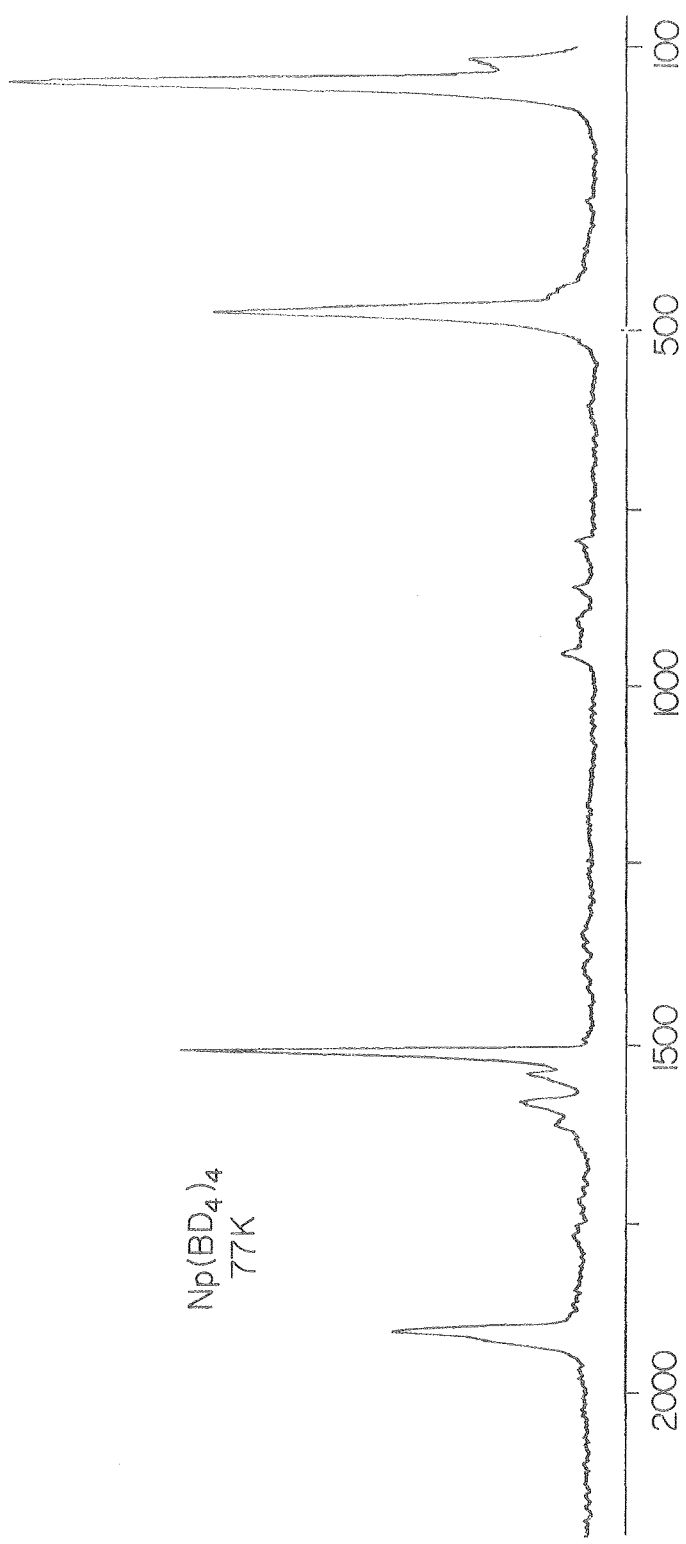
Np(BD$_4$)$_4$
77K

Wavenumber (cm^{-1})

Figure 5.

XBL 795 - 1877
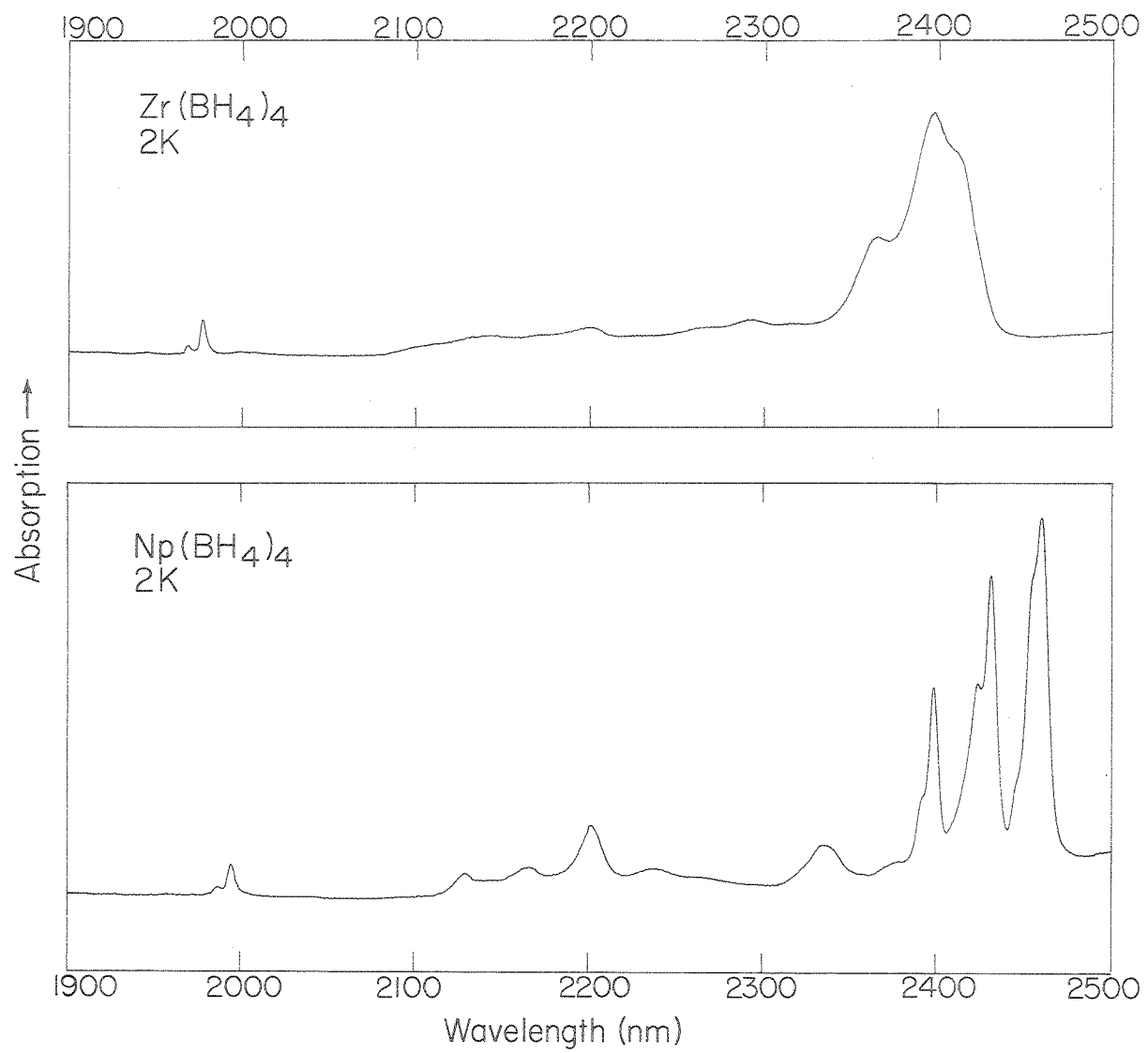
Figure 6.

XBL 798-2703
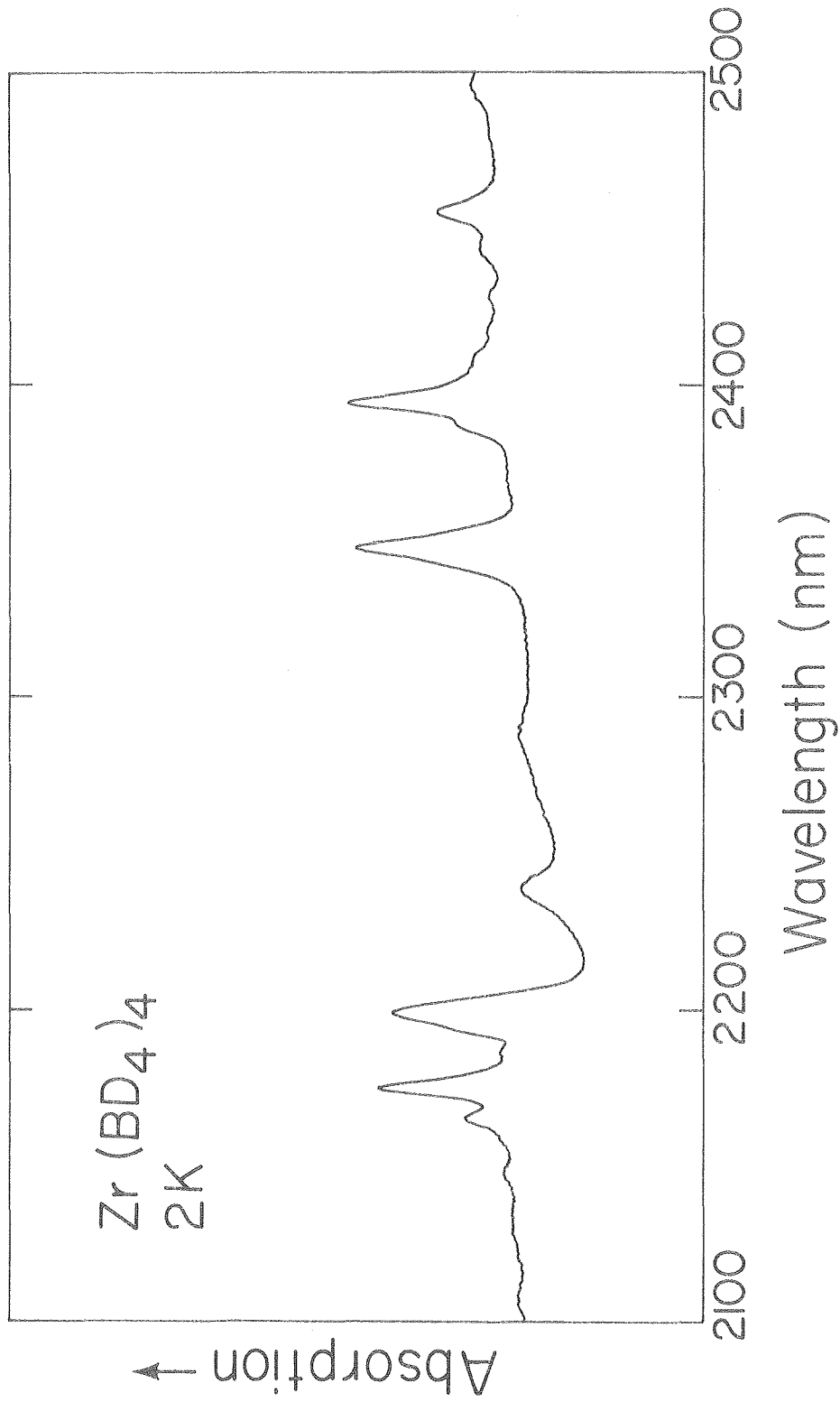
Figure 7.

$Zr(BD_4)_4$
2K

Absorption →

Wavelength (nm)

2100 2200 2300 2400 2500

XBL 798-2701

TECHNICAL INFORMATION DEPARTMENT
LAWRENCE BERKELEY LABORATORY
UNIVERSITY OF CALIFORNIA
BERKELEY, CALIFORNIA 94720